5

Actuators and Sensors

In this chapter, two basic robot components are treated: *actuators* and *sensors*. In the first part, the features of an *actuating system* are presented in terms of the power supply, power amplifier, servomotor and transmission. In view of their control versatility, two types of servomotors are used, namely, *electric servomotors* for actuating the joints of small and medium size manipulators, and *hydraulic servomotors* for actuating the joints of large size manipulators. The models describing the input/output relationship for such servomotors are derived, together with the control schemes of the *drives*. The electric servomotors are also employed to actuate the wheels of the mobile robots, which will be dealt with in Chap. 11. Successively, *proprioceptive sensors* are presented which allow measurement of the quantities characterizing the internal state of the manipulator, namely, *encoders* and *resolvers* for joint position measurement, *tachometers* for joint velocity measurement; further, *exteroceptive sensors* are presented including *force sensors* for end-effector force measurement, *distance sensors* for detection of objects in the workspace, and *vision sensors* for the measurement of the characteristic parameters of such objects, whenever the manipulator interacts with the environment.

5.1 Joint Actuating System

The motion imposed to a manipulator's joint is realized by an *actuating system* which in general consists of:

- a *power supply*,
- a *power amplifier*,
- a *servomotor*,
- a *transmission*.

The connection between the various components is illustrated in Fig. 5.1 where the exchanged powers are shown. To this end, recall that power can

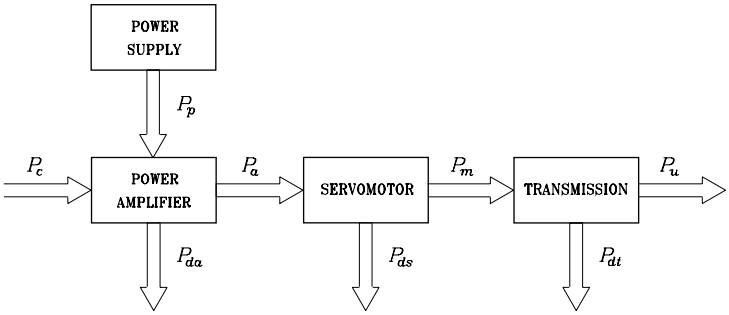

Fig. 5.1. Components of a joint actuating system

always be expressed as the product of a flow and a force quantity, whose physical context allows the specification of the nature of the power (mechanical, electric, hydraulic, or pneumatic).

In terms of a global input/output relationship, P_c denotes the (usually electric) power associated with the control law signal, whereas P_u represents the mechanical power required to the joint to actuate the motion. The intermediate connections characterize the supply power P_a of the motor (of electric, hydraulic, or pneumatic type), the power provided by the primary source P_p of the same physical nature as that of P_a, and the mechanical power P_m developed by the motor. Moreover, P_{da}, P_{ds} and P_{dt} denote the powers lost for dissipation in the conversions performed respectively by the amplifier, motor and transmission.

To choose the components of an actuating system, it is worth starting from the requirements imposed on the mechanical power P_u by the force and velocity that describe the joint motion.

5.1.1 Transmissions

The execution of joint motions of a manipulator demands *low speeds* with *high torques*. In general, such requirements do not allow an effective use of the mechanical features of servomotors, which typically provide high speeds with low torques in optimal operating conditions. It is then necessary to interpose a *transmission* (*gear*) to optimize the transfer of mechanical power from the motor (P_m) to the joint (P_u). During this transfer, the power P_{dt} is dissipated as a result of friction.

The choice of the transmission depends on the power requirements, the kind of desired motion, and the allocation of the motor with respect to the joint. In fact, the transmission allows the outputs of the motor to be transformed both quantitatively (velocity and torque) and qualitatively (a rotational motion about the motor axis into a translational motion of the joint). Also, it allows the static and dynamic performance of a manipulator to be optimized, by reducing the effective loads when the motor is located upstream

of the joint; for instance, if some motors are mounted to the base of the robot, the total weight of the manipulator is decreased and the power-to-weight ratio is increased.

The following transmissions are typically used for industrial robots:

- *Spur gears* that modify the characteristics of the rotational motion of the motor by changing the axis of rotation and/or by translating the application point; spur gears are usually constructed with wide cross-section teeth and squat shafts.
- *Lead screws* that convert rotational motion of the motor into translational motion, as needed for actuation of prismatic joints; in order to reduce friction, ball screws are usually employed that are preloaded so as to increase stiffness and decrease backlash.
- *Timing belts* and *chains* which are equivalent from a kinematic viewpoint and are employed to locate the motor remotely from the axis of the actuated joint. The stress on timing belts may cause strain, and then these are used in applications requiring high speeds and low forces. On the other hand, chains are used in applications requiring low speeds, since their large mass may induce vibration at high speeds.

On the assumption of rigid transmissions with no backlash, the relationship between input forces (velocities) and output forces (velocities) is purely proportional.

The mechanical features of the motor used for an actuating system may sometimes allow a direct connection of the motor to the joint without the use of any transmission element (*direct drive*). The drawbacks due to transmission elasticity and backlash are thus eliminated, although more sophisticated control algorithms are required, since the absence of reduction gears does not allow the nonlinear coupling terms in the dynamic model to be neglected. The use of direct-drive actuating systems is not yet popular for industrial manipulators, in view of the cost and size of the motors as well as of control complexity.

5.1.2 Servomotors

Actuation of joint motions is entrusted to *motors* which allow the realization of a desired motion for the mechanical system. Concerning the kind of input power P_a, motors can be classified into three groups:

- *Pneumatic motors* which utilize the pneumatic energy provided by a compressor and transform it into mechanical energy by means of pistons or turbines.
- *Hydraulic motors* which transform the hydraulic energy stored in a reservoir into mechanical energy by means of suitable pumps.
- *Electric motors* whose primary supply is the electric energy available from the electric distribution system.

A portion of the input power P_a is converted to output as mechanical power P_m, and the rest (P_{ds}) is dissipated because of mechanical, electric, hydraulic, or pneumatic loss.

The motors employed in robotics are the evolution of the motors employed in industrial automation having powers ranging from about 10 W to about 10 kW. For the typical performance required, such motors should have the following requirements with respect to those employed in conventional applications:

- low inertia and high power-to-weight ratio,
- possibility of overload and delivery of impulse torques,
- capability to develop high accelerations,
- wide velocity range (from 1 to 1000 revolutes/min),
- high positioning accuracy (at least 1/1000 of a circle),
- low torque ripple so as to guarantee continuous rotation even at low speed.

These requirements are enhanced by the good trajectory tracking and positioning accuracy demanded for an actuating system for robots, and thus the motor must play the role of a *servomotor*. In this respect, pneumatic motors are difficult to control accurately, in view of the unavoidable fluid compressibility errors. Therefore, they are not widely employed, if not for the actuation of the typical opening and closing motions of the jaws in a gripper tool, then for the actuation of simple arms used in applications where continuous motion control is not of concern.

The most employed motors in robotics applications are *electric servomotors*. Among them, the most popular are permanent-magnet direct-current (DC) servomotors and brushless DC servomotors, in view of their good control flexibility.

The *permanent-magnet DC servomotor* consists of:

- A stator coil that generates magnetic flux; this generator is always a permanent magnet made by ferromagnetic ceramics or rare earths (high fields in contained space).
- An armature that includes the current-carrying winding that surrounds a rotary ferromagnetic core (rotor).
- A commutator that provides an electric connection by means of brushes between the rotating armature winding and the external feed winding, according to a commutation logic determined by the rotor motion.

The *brushless DC servomotor* consists of:

- A rotating coil (rotor) that generates magnetic flux; this generator is a permanent magnet made by ferromagnetic ceramics or rare earths.
- A stationary armature (stator) made by a polyphase winding.
- A static commutator that, on the basis of the signals provided by a position sensor located on the motor shaft, generates the feed sequence of the armature winding phases as a function of the rotor motion.

With reference to the above details of constructions, a comparison between the operating principle of a permanent-magnet DC and a brushless DC servomotor leads to the following considerations.

In the brushless DC motor, by means of the rotor position sensor, the winding orthogonal to the magnetic field of the coil is found; then, feeding the winding makes the rotor rotate. As a consequence of rotation, the electronic control module commutes the feeding on the winding of the various phases in such a way that the resulting field at the armature is always kept orthogonal to that of the coil. As regards electromagnetic interaction, such a motor operates in a way similar to that of a permanent-magnet DC motor where the brushes are at an angle of $\pi/2$ with respect to the direction of the excitation flux. In fact, feeding the armature coil makes the rotor rotate, and commutation of brushes from one plate of the commutator to the other allows the rotor to be maintained in rotation. The role played by the brushes and commutator in a permanent-magnet DC motor is analogous to that played by the position sensor and electronic control module in a brushless DC motor.

The main reason for using a brushless DC motor is to eliminate the problems due to mechanical commutation of the brushes in a permanent-magnet DC motor. In fact, the presence of the commutator limits the performance of a permanent-magnet DC motor, since this provokes electric loss due to voltage drops at the contact between the brushes and plates, and mechanical loss due to friction and arcing during commutation from one plate to the next one caused by the inductance of the winding. The elimination of the causes provoking such inconveniences, i.e., the brushes and plates, allows an improvement of motor performance in terms of higher speeds and less material wear.

The inversion between the functions of stator and rotor leads to further advantages. The presence of a winding on the stator instead of the rotor facilitates heat disposal. The absence of a rotor winding, together with the possibility of using rare-earth permanent magnets, allows construction of more compact rotors which are, in turn, characterized by a low moment of inertia. Therefore, the size of a brushless DC motor is smaller than that of a permanent-magnet DC motor of the same power; an improvement of dynamic performance can also be obtained by using a brushless DC motor. For the choice of the most suitable servomotor for a specific application, the cost factor plays a relevant role.

Not uncommon are also stepper motors. These actuators are controlled by suitable excitation sequences and their operating principle does not require measurement of motor shaft angular position. The dynamic behaviour of stepper motors is greatly influenced by payload, though. Also, they induce vibration of the mechanical structure of the manipulator. Such inconveniences confine the use of stepper motors to the field of micromanipulators, for which low-cost implementation prevails over the need for high dynamic performance.

A certain number of applications features the employment of *hydraulic servomotors*, which are based on the simple operating principle of volume

variation under the action of compressed fluid. From a construction viewpoint, they are characterized by one or more chambers made by pistons (cylinders reciprocating in tubular housings). Linear servomotors have a limited range and are constituted by a single piston. Rotary servomotors have unlimited range and are constituted by several pistons (usually an odd number) with an axial or radial disposition with respect to the motor axis of rotation. These servomotors offer a static and dynamic performance comparable with that offered by electric servomotors.

The differences between electric and hydraulic servomotors can be fundamentally observed from a plant viewpoint. In this respect, *electric servomotors* present the following *advantages*:

- widespread availability of power supply,
- low cost and wide range of products,
- high power conversion efficiency,
- easy maintenance,
- no pollution of working environment.

Instead, they present the following *limitations*:

- burnout problems at static situations caused by the effect of gravity on the manipulator; emergency brakes are then required,
- need for special protection when operating in flammable environments.

Hydraulic servomotors present the following *drawbacks*:

- need for a hydraulic power station,
- high cost, narrow range of products, and difficulty of miniaturization,
- low power conversion efficiency,
- need for operational maintenance,
- pollution of working environment due to oil leakage.

In their *favour* it is worth pointing out that they:

- do not suffer from burnout in static situations,
- are self-lubricated and the circulating fluid facilitates heat disposal,
- are inherently safe in harmful environments,
- have excellent power-to-weight ratios.

From an operational viewpoint, it can be observed that:

- Both types of servomotors have a good dynamic behaviour, although the electric servomotor has greater control flexibility. The dynamic behaviour of a hydraulic servomotor depends on the temperature of the compressed fluid.
- The electric servomotor is typically characterized by high speeds and low torques, and as such it requires the use of gear transmissions (causing elasticity and backlash). On the other hand, the hydraulic servomotor is capable of generating high torques at low speeds.

In view of the above remarks, hydraulic servomotors are specifically employed for manipulators that have to carry heavy payloads; in this case, not only is the hydraulic servomotor the most suitable actuator, but also the cost of the plant accounts for a reduced percentage on the total cost of the manipulation system.

5.1.3 Power Amplifiers

The *power amplifier* has the task of modulating, under the action of a control signal, the power flow which is provided by the primary supply and has to be delivered to the actuators for the execution of the desired motion. In other words, the amplifier takes a fraction of the power available at the source which is proportional to the control signal; then it transmits this power to the motor in terms of suitable force and flow quantities.

The inputs to the amplifier are the power taken from the primary source P_p and the power associated with the control signal P_c. The total power is partly delivered to the actuator (P_a) and partly lost in dissipation (P_{da}).

Given the typical use of electric and hydraulic servomotors, the operational principles of the respective amplifiers are discussed.

To control an *electric servomotor*, it is necessary to provide it with a voltage or current of suitable form depending on the kind of servomotor employed. Voltage (or current) is direct for permanent-magnet DC servomotors, while it is alternating for brushless DC servomotors. The value of voltage for permanent-magnet DC servomotors or the values of voltage and frequency for brushless DC servomotors are determined by the control signal of the amplifier, so as to make the motor execute the desired motion.

For the power ranges typically required by joint motions (of the order of a few kilowatts), transistor amplifiers are employed which are suitably switched by using pulse-width modulation (PWM) techniques. They allow the achievement of a power conversion efficiency $P_a/(P_p + P_c)$ greater than 0.9 and a power gain P_a/P_c of the order of 10^6. The amplifiers employed to control permanent-magnet DC servomotors are DC-to-DC converters (*choppers*), whereas those employed to control brushless DC servomotors are DC-to-AC converters (*inverters*).

Control of a *hydraulic servomotor* is performed by varying the flow rate of the compressed fluid delivered to the motor. The task of modulating the flow rate is typically entrusted to an interface (electro-hydraulic servovalve). This allows a relationship to be established between the electric control signal and the position of a distributor which is able to vary the flow rate of the fluid transferred from the primary source to the motor. The electric control signal is usually current-amplified and feeds a solenoid which moves (directly or indirectly) the distributor, whose position is measured by a suitable transducer. In this way, a position servo on the valve stem is obtained which reduces occurrence of any stability problem that may arise on motor control. The magnitude of the control signal determines the flow rate of the compressed

fluid through the distributor, according to a characteristic which is possibly made linear by means of a keen mechanical design.

5.1.4 Power Supply

The task of the *power supply* is to supply the primary power to the amplifier which is needed for operation of the actuating system.

In the case of *electric servomotors*, the power supply consists of a transformer and a typically uncontrolled bridge rectifier. These allow the alternating voltage available from the distribution to be converted into a direct voltage of suitable magnitude which is required to feed the power amplifier.

In the case of *hydraulic servomotors*, the power supply is obviously more complex. In fact, a gear or piston pump is employed to compress the fluid which is driven by a primary motor operating at constant speed, typically a three-phase nonsynchronous motor. To reduce the unavoidable pressure oscillations provoked by a flow rate demand depending on operational conditions of the motor, a reservoir is interfaced to store hydraulic energy. Such a reservoir, in turn, plays the same role as the filter capacitor used at the output of a bridge rectifier. The hydraulic power station is completed by the use of various components (filters, pressure valves, and check valves) that ensure proper operation of the system. Finally, it can be inferred how the presence of complex hydraulic circuits operating at high pressures (of the order of 100 atm) causes an appreciable pollution of the working environment.

5.2 Drives

This section presents the operation of the *electric drives* and the *hydraulic drives* for the actuation of a manipulator's joints. Starting from the mathematical models describing the dynamic behaviour, the block schemes are derived which allow an emphasis on the control features and the effects of the use of a mechanical transmission.

5.2.1 Electric Drives

From a modelling viewpoint, a permanent-magnet DC motor and a brushless DC motor provided with the commutation module and position sensor can be described by the same differential equations. In the domain of the complex variable s, the electric balance of the armature is described by the equations

$$V_a = (R_a + sL_a)I_a + V_g \tag{5.1}$$

$$V_g = k_v \Omega_m \tag{5.2}$$

where V_a and I_a respectively denote armature voltage and current, R_a and L_a are respectively the armature resistance and inductance, and V_g denotes

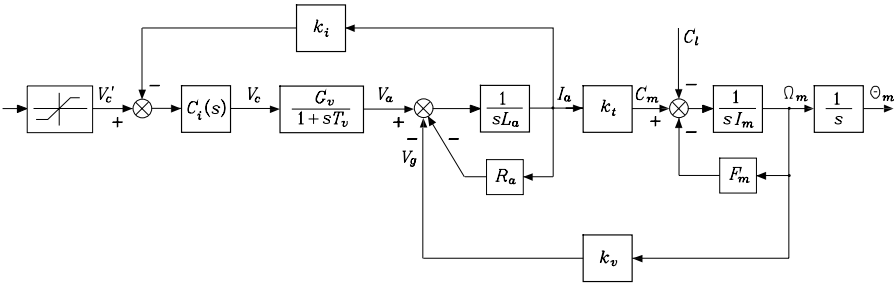

Fig. 5.2. Block scheme of an electric drive

the back electromotive force which is proportional to the angular velocity Ω_m through the voltage constant k_v that depends on the construction details of the motor as well as on the magnetic flux of the coil.

The mechanical balance is described by the equations

$$C_m = (sI_m + F_m)\Omega_m + C_l \tag{5.3}$$

$$C_m = k_t I_a \tag{5.4}$$

where C_m and C_l respectively denote the driving torque and load reaction torque, I_m and F_m are respectively the moment of inertia and viscous friction coefficient at the motor shaft, and the torque constant k_t is numerically equal to k_v in the SI unit system for a compensated motor.

Concerning the power amplifier, the input/output relationship between the control voltage V_c and the armature voltage V_a is given by the transfer function

$$\frac{V_a}{V_c} = \frac{G_v}{1 + sT_v} \tag{5.5}$$

where G_v denotes the voltage gain and T_v is a time constant that can be neglected with respect to the other time constants of the system. In fact, by using a modulation frequency in the range of 10 to 100 kHz, the time constant of the amplifier is in the range of 10^{-5} to 10^{-4}) s.

The block scheme of the servomotor with power amplifier (*electric drive*) is illustrated in Fig. 5.2. In such a scheme, besides the blocks corresponding to the above relations, there is an armature *current feedback* loop where current is thought of as measured by a transducer k_i between the power amplifier and the armature winding of the motor. Further, the scheme features a current regulator $C_i(s)$ as well as an element with a nonlinear saturation characteristic. The aim of such feedback is twofold. On one hand, the voltage V_c' plays the role of a current reference and thus, by means of a suitable choice of the regulator $C_i(s)$, the lag between the current I_a and the voltage V_c' can be reduced with respect to the lag between I_a and V_c. On the other hand, the introduction of a saturation nonlinearity allows the limitation of the magni-

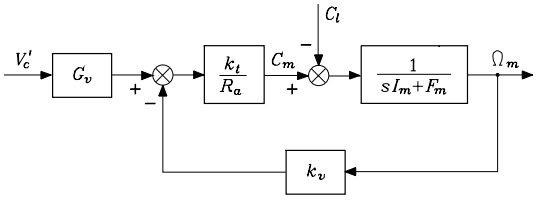

Fig. 5.3. Block scheme of an electric drive as a velocity-controlled generator

tude of V_c', and then it works like a current limit which ensures protection of the power amplifier whenever abnormal operating conditions occur.

The choice of the regulator $C_i(s)$ of the current loop allows a velocity-controlled or torque-controlled behaviour to be obtained from the electric drive, depending on the values attained by the loop gain. In fact, in the case of $k_i = 0$, recalling that the mechanical viscous friction coefficient is negligible with respect to the electrical friction coefficient

$$F_m \ll \frac{k_v k_t}{R_a}, \tag{5.6}$$

assuming a unit gain constant for $C_i(s)$[1] and $C_l = 0$ yields

$$\omega_m \approx \frac{G_v}{k_v} v_c' \tag{5.7}$$

and thus the drive system behaves like a *velocity-controlled generator*.

Instead, when $k_i \neq 0$, choosing a large loop gain for the current loop ($Kk_i \gg R_a$) leads at steady state to

$$c_m \approx \frac{k_t}{k_i} \left(v_c' - \frac{k_v}{G_v} \omega_m \right); \tag{5.8}$$

the drive behaves like a *torque-controlled generator* since, in view of the large value of G_v, the driving torque is practically independent of the angular velocity.

As regards the dynamic behaviour, it is worth considering a *reduced-order model* which can be obtained by neglecting the electric time constant L_a/R_a with respect to the mechanical time constant I_m/F_m, assuming $T_v \approx 0$ and a purely proportional controller. These assumptions, together with $k_i = 0$, lead to the block scheme in Fig. 5.3 for the velocity-controlled generator. On the other hand, if it is assumed $Kk_i \gg R_a$ and $k_v \Omega / Kk_i \approx 0$, the resulting block scheme of the torque-controlled generator is that in Fig. 5.4. From the

[1] It is assumed $C_i(0) = 1$; in the case of presence of an integral action in $C_i(s)$, it should be $\lim_{s \to 0} sC(s) = 1$.

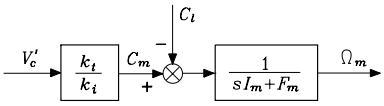

Fig. 5.4. Block scheme of an electric drive as a torque-controlled generator

above schemes, the following input/output relations between control voltage, reaction torque, and angular velocity can be derived:

$$\Omega_m = \frac{\dfrac{1}{k_v}}{1 + s\dfrac{R_a I_m}{k_v k_t}} G_v V_c' - \frac{\dfrac{R_a}{k_v k_t}}{1 + s\dfrac{R_a I_m}{k_v k_t}} C_l \tag{5.9}$$

for the velocity-controlled generator, and

$$\Omega_m = \frac{\dfrac{k_t}{k_i F_m}}{1 + s\dfrac{I_m}{F_m}} V_c' - \frac{\dfrac{1}{F_m}}{1 + s\dfrac{I_m}{F_m}} C_l \tag{5.10}$$

for the torque-controlled generator. These transfer functions show how, without current feedback, the system has a better rejection of disturbance torques in terms of both equivalent gain ($R_a/k_v k_t \ll 1/F_m$) and time response ($R_a I_m/k_v k_t \ll I_m/F_m$).

The relationship between the control input and the actuator position output can be expressed in a unified manner by the transfer function

$$M(s) = \frac{k_m}{s(1 + sT_m)} \tag{5.11}$$

where

$$k_m = \frac{1}{k_v} \qquad T_m = \frac{R_a I_m}{k_v k_t} \tag{5.12}$$

for the velocity-controlled generator, while for the torque-controlled generator it is

$$k_m = \frac{k_t}{k_i F_m} \qquad T_m = \frac{I_m}{F_m}. \tag{5.13}$$

Notice how the power amplifier, in the velocity control case, contributes to the input/output relation with the constant G_v, while in the case of current control the amplifier, being inside a local feedback loop, does not appear as a stand alone but rather in the expression of k_m with a factor $1/k_i$.

These considerations lead to the following conclusions. In all such applications where the drive system has to provide high rejection of disturbance torques (as in the case of independent joint control, see Sect. 8.3) it is not advisable to have a current feedback in the loop, at least when all quantities

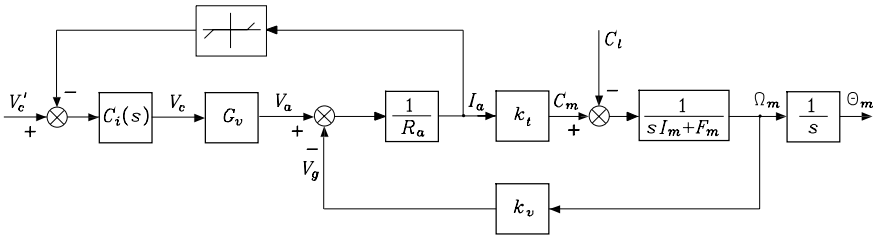

Fig. 5.5. Block scheme of an electric drive with nonlinear current feedback

are within their nominal values. In this case, the problem of setting a protection can be solved by introducing a current limit that is not performed by a saturation on the control signal but it exploits a current feedback with a dead-zone nonlinearity on the feedback path, as shown in Fig. 5.5. Therefore, an actual current limit is obtained whose precision is as high as the slope of the dead zone; it is understood that stability of the current loop is to be addressed when operating in this way.

As will be shown in Sect. 8.5, centralized control schemes, instead, demand the drive system to behave as a torque-controlled generator. It is then clear that a current feedback with a suitable regulator $C_i(s)$ should be used so as to confer a good static and dynamic behaviour to the current loop. In this case, servoing of the driving torque is achieved indirectly, since it is based on a current measurement which is related to the driving torque by means of gain $1/k_t$.

5.2.2 Hydraulic Drives

No matter how a hydraulic servomotor is constructed, the derivation of its input/output mathematical model refers to the basic equations describing the relationship between flow rate and pressure, the relationship between the fluid and the parts in motion, and the mechanical balance of the parts in motion. Let Q represent the volume flow rate supplied by the distributor; the flow rate balance is given by the equation

$$Q = Q_m + Q_l + Q_c \tag{5.14}$$

where Q_m is the flow rate transferred to the motor, Q_l is the flow rate due to leakage, and Q_c is the flow rate related to fluid compressibility. The terms Q_l and Q_c are taken into account in view of the high operating pressures (of the order of 100 atm).

Let P denote the differential pressure of the servomotor due to the load; then it can be assumed that

$$Q_l = k_l P. \tag{5.15}$$

Regarding the loss for compressibility, if V denotes the instantaneous volume of the fluid, one has

$$Q_c = \gamma V s P \tag{5.16}$$

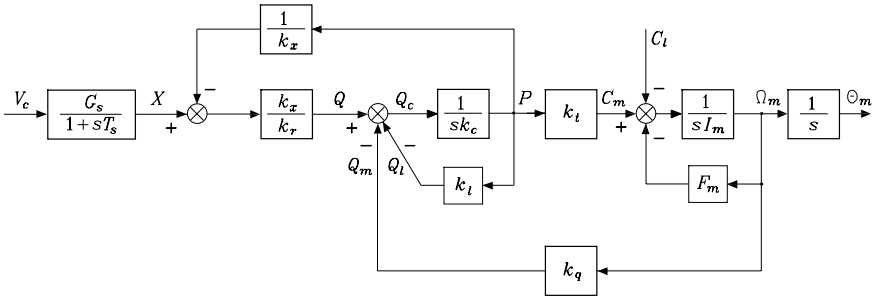

Fig. 5.6. Block scheme of a hydraulic drive

where γ is the uniform compressibility coefficient of the fluid. Notice that the proportional factor $k_c = \gamma V$ between the time derivative of the pressure and the flow rate due to compressibility depends on the volume of the fluid; therefore, in the case of rotary servomotors, k_c is a constant, whereas in the case of a linear servomotor, the volume of fluid varies and thus the characteristic of the response depends on the operating point.

The volume flow rate transferred to the motor is proportional to the volume variation in the chambers per time unit; with reference from now on to a rotary servomotor, such variation is proportional to the angular velocity, and then

$$Q_m = k_q \Omega_m. \tag{5.17}$$

The mechanical balance of the parts in motion is described by

$$C_m = (sI_m + F_m)\Omega_m + C_l \tag{5.18}$$

with obvious meaning of the symbols. Finally, the driving torque is proportional to the differential pressure of the servomotor due to the load, i.e.,

$$C_m = k_t P. \tag{5.19}$$

Concerning the servovalve, the transfer function between the stem position X and the control voltage V_c is expressed by

$$\frac{X}{V_c} = \frac{G_s}{1 + sT_s} \tag{5.20}$$

thanks to the linearizing effect achieved by position feedback; G_s is the equivalent gain of the servovalve, whereas its time constant T_s is of the order of ms and thus it can be neglected with respect to the other time constants of the system.

Finally, regarding the distributor, the relationship between the differential pressure, the flow rate, and the stem displacement is highly nonlinear; linearization about an operating point leads to the equation

$$P = k_x X - k_r Q. \tag{5.21}$$

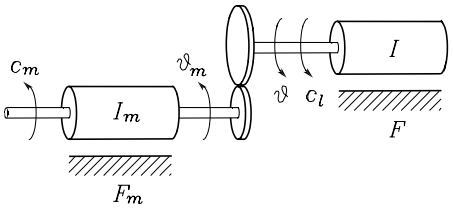

Fig. 5.7. Schematic representation of a mechanical gear

By virtue of (5.14)–(5.21), the servovalve/distributor/motor complex (*hydraulic drive*) is represented by the block scheme of Fig. 5.6. A comparison between the schemes in Figs. 5.2 and 5.6 clearly shows the formal analogy in the dynamic behaviour of an electric and a hydraulic servomotor. Nevertheless, such analogy should not induce one to believe that it is possible to make a hydraulic drive play the role of a velocity- or torque-controlled generator, as for an electric drive. In this case, the pressure feedback loop (formally analogous to the current feedback loop) is indeed a structural characteristic of the system and, as such, it cannot be modified but with the introduction of suitable transducers and the realization of the relative control circuitry.

5.2.3 Transmission Effects

In order to describe quantitatively the effects introduced by the use of a transmission (*mechanical gear*) between the servomotor and the actuated joint, it is worth referring to the mechanical coupling realized by a pair of spur gears of radius r_m and r, which is schematically represented in Fig. 5.7; the kinematic pair is assumed to be ideal (without backlash) and connects the rotation axis of the servomotor with the axis of the corresponding joint.

With reference to an electric servomotor, it is assumed that the rotor of the servomotor is characterized by an inertia moment I_m about its rotation axis and a viscous friction coefficient F_m; likewise, I and F denote the inertia moment and the viscous friction coefficient of the load. The inertia moments and the friction coefficients of the gears are assumed to have been included in the corresponding parameters of the motor (for the gear of radius r_m) and of the load (for the gear of radius r). Let c_m denote the driving torque of the motor and c_l the reaction torque applied to the load axis. Also let ω_m and ϑ_m denote the angular velocity and position of the motor axis, while ω and ϑ denote the corresponding quantities at the load side. Finally, f indicates the force exchanged at the contact between the teeth of the two gears.[2]

[2] In the case considered, it has been assumed that both the motor and the load are characterized by revolute motions; if the load should exhibit a translation motion, the following arguments can be easily extended, with analogous results, by replacing the angular displacements with linear displacements and the inertia moments with masses at the load side.

The gear reduction ratio is defined as

$$k_r = \frac{r}{r_m} = \frac{\vartheta_m}{\vartheta} = \frac{\omega_m}{\omega} \tag{5.22}$$

since, in the absence of slipping in the kinematic coupling, it is $r_m \vartheta_m = r\vartheta$.

The gear reduction ratio, in the case when it is representative of the coupling between a servomotor and the joint of a robot manipulator, attains values much larger than unity ($r_m \ll r$) — typically from a few tens to a few hundreds.

The force f exchanged between the two gears generates a reaction torque $f \cdot r_m$ for the motion at the motor axis and a driving torque $f \cdot r$ for the rotation motion of the load.

The mechanical balances at the motor side and the load side are respectively:

$$c_m = I_m \dot{\omega}_m + F_m \omega_m + f r_m \tag{5.23}$$

$$fr = I\dot{\omega} + F\omega + c_l. \tag{5.24}$$

To describe the motion with reference to the motor angular velocity, in view of (5.22), combining the two equations gives at the motor side

$$c_m = I_{eq} \dot{\omega}_m + F_{eq} \omega_m + \frac{c_l}{k_r} \tag{5.25}$$

where

$$I_{eq} = \left(I_m + \frac{I}{k_r^2} \right) \qquad F_{eq} = \left(F_m + \frac{F}{k_r^2} \right). \tag{5.26}$$

The expressions (5.25), (5.26) show how, in the case of a gear with large reduction ratio, the inertia moment and the viscous friction coefficient of the load are reflected at the motor axis with a reduction of a factor $1/k_r^2$; the reaction torque, instead, is reduced by a factor $1/k_r$. If this torque depends on ϑ in a nonlinear fashion, then the presence of a large reduction ratio tends to linearize the dynamic equation.

Example 5.1

In Fig. 5.8 a rigid pendulum is represented, which is actuated by the torque $f \cdot r$ to the load axis after the gear. In this case, the dynamic equations of the system are

$$c_m = I_m \dot{\omega}_m + F_m \omega_m + f r_m \tag{5.27}$$

$$fr = I\dot{\omega} + F\omega + mg\ell \sin\vartheta \tag{5.28}$$

where I is the inertia moment of the pendulum at the load axis, F is the viscous friction coefficient, m is the pendulum mass, ℓ its length and g the gravity acceleration. Reporting (5.28) to the motor axis gives

$$c_m = I_{eq} \dot{\omega}_m + F_{eq} \omega_m + \left(\frac{mg\ell}{k_r} \right) \sin\left(\frac{\vartheta_m}{k_r} \right) \tag{5.29}$$

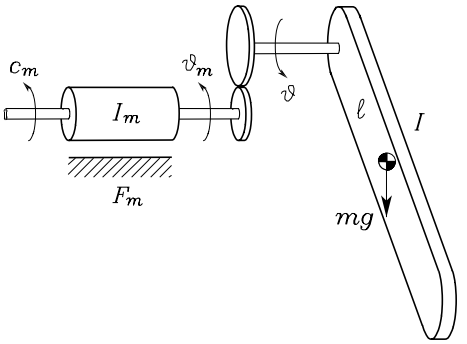

Fig. 5.8. Pendulum actuated via mechanical gear

from which it is clear how the contribution of the nonlinear term is reduced by the factor k_r.

The example of the pendulum has been considered to represent an n-link manipulator with revolute joints, for which each link, considered as isolated from the others, can be considered as a simple rigid pendulum. The connection with other links introduces, in reality, other nonlinear effects which complicate the input/output model; in this regard, it is sufficient to notice that, in the case of a double pendulum, the inertia moment at the motor side of the first link depends also on the angular position of the second link.

In Chap. 7 the effect introduced by the presence of transmissions in a generic n-link manipulator structure will be studied in detail. Nevertheless, it can already be understood how the nonlinear couplings between the motors of the various links will be reduced by the presence of transmissions with large reduction ratios.

5.2.4 Position Control

After having examined the modalities to control the angular velocity of an electric or hydraulic drive, the motion control problem for a link of a generic manipulator is to be solved. A structure is sought which must be capable of determining, in an automatic way, the time evolution of the quantity chosen to control the drive, so that the actuated joint executes the required motion allowing the end-effector to execute a given task.

Once a trajectory has been specified for the end-effector pose, the solution of the inverse kinematics problem allows the computation of the desired trajectories for the various joints, which thus can be considered as available.

Several control techniques can be adopted to control the manipulator motion; the choice of a particular solution depends on the required dynamic performance, the kind of motion to execute, the kinematic structure, and the

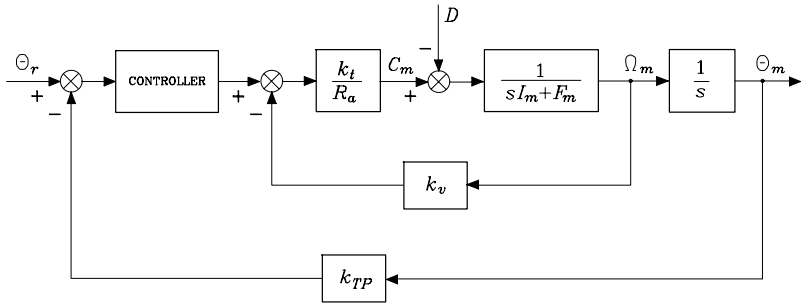

Fig. 5.9. General block scheme of electric drive control

choice to utilize either servomotors with transmissions or torque motors with joint direct drive.

The simplest solution is to consider, at first approximation, the motion of a joint independent of the motion of the other joints, i.e., the interaction can be regarded as a disturbance. Assume the reference trajectory $\vartheta_r(t)$ is available. According to classical automatic control theory, to ensure that the angular motor position ϑ_m, properly measured by means of a transducer with constant k_{TP}, follows ϑ_r, it is worth resorting to a feedback control system providing 'robustness' with respect to both model uncertainty on the motor and the load, and the presence of a disturbance. A more detailed treatment is deferred to Chap. 8, where the most congenial solutions to solve the above problems will be presented.

In the following, the problem of joint *position control* is tackled by assuming an electric DC servomotor; the choice is motivated by the diffusion of this technology, due to the high flexibility of these actuators providing optimal responses in the large majority of motion control applications.

The choice of a feedback control system to realize a position servo at the motor axis requires the adoption of a *controller*; this device generates a signal which, applied to the power amplifier, automatically generates the driving torque producing an axis motion very close to the desired motion ϑ_r. Its structure should be so that the error between the reference input and the measured output is minimized, even in the case of inaccurate knowledge of the dynamics of the motor, the load, and a disturbance. The *rejection* action of the disturbance is the more efficient, the smaller the magnitude of the disturbance.

On the other hand, according to (5.9), the disturbance is minimized, provided the drive is velocity-controlled. In this case, in view of (5.6), the reaction torque influences the motor axis velocity with a coefficient equal to $R_a/k_v k_t$ which is much smaller than $1/F_m$, which represents instead the weight on the reaction torque in the case when the drive is torque-controlled. Therefore, with reference to Fig. 5.3, the general scheme of drive control with *position feedback* is illustrated in Fig. 5.9, where the disturbance d represents the load

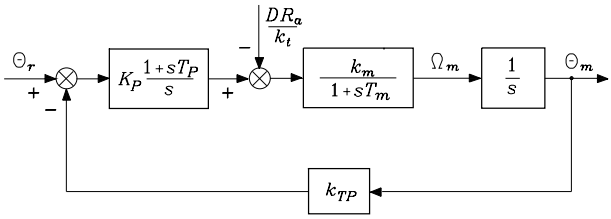

Fig. 5.10. Block scheme of drive control with position feedback

torque and the value of the power amplifier gain has been included in the control action.

Besides reducing the effects of the disturbance on the output, the structure of the controller must ensure an optimal trade-off between the stability of the feedback control system and the capability of the output to dynamically track the reference with a reduced error.

The reduction of the disturbance effects on the output can be achieved by conferring a large value of the gain before the point of intervention of the disturbance, without affecting stability. If, at steady state (ϑ_r = cost, c_l = cost), it is desired to cancel the disturbance effect on the output, the controller must act an *integral action* on the error given by the difference between ϑ_r and $k_{TP}\vartheta_m$.

The above requirements suggest the use of a simple controller with an integral and a proportional action on the error; the *proportional action* is added to realize a stabilizing action, which, however, cannot confer to the closed-loop system a damped transient response with a sufficiently short sampling time. This behaviour is due to the presence of a double pole at the origin of the transfer function of the forward path.

The resulting control scheme is illustrated in Fig. 5.10, where k_m and T_m are respectively the voltage-to-velocity gain constant and the characteristic time constant of the motor in (5.12). The parameters of the controller K_P and T_P should be keenly chosen so as to ensure stability of the feedback control system and obtain a good dynamic behaviour.

To improve the transient response, the industrial drives employed for position servoing may also include a local feedback loop based on the angular velocity measurement (tachometer feedback). The general scheme with *position and velocity feedback* is illustrated in Fig. 5.11; besides the position transducer, a velocity transducer is used with constant k_{TV}, as well as a simple proportional controller with gain K_P. With the adoption of the tachometer feedback, the proportional-integral controller with parameters K_V and T_V is retained in the internal velocity loop so as to cancel the effects of the disturbance on the position ϑ_m at steady state. The presence of two feedback loops, in lieu of one, around the intervention point of the disturbance is expected to lead to a further reduction of the disturbance effects on the output also during the transients.

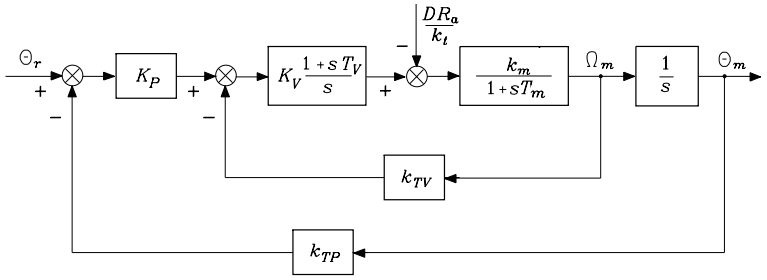

Fig. 5.11. Block scheme of drive control with position and velocity feedback

The adoption of tachometer feedback may also improve the transient response of the whole control system with respect to the previous case. With a keen choice of the controller parameters, indeed, it is possible to achieve a transfer function between ϑ_m and ϑ_r with a larger bandwidth and reduced resonance phenomena. The result is a faster transient response with reduced oscillations, thus improving the capability of $\vartheta_m(t)$ to track more demanding reference trajectories $\vartheta_r(t)$.

The above analysis will be further detailed in Sect. 8.3.

The position servo may also utilize a current-controller motor; the schemes in Figs. 5.9–5.11 can be adopted, provided that the constants in (5.13) are used in the transfer function (5.11) and the disturbance D is weighed with the quantity k_i/k_t in lieu of R_a/k_t. In that case, the voltage gain G_v of the power amplifier will not contribute to the control action.

As a final consideration, the general control structure presented above may be extended to the case when the motor is coupled to a load via a gear reduction. In such a case, it is sufficient to account for (5.25) and (5.26), i.e., replace I_m and F_m with the quantities I_{eq} and F_{eq}, and scale the disturbance by the factor $1/k_r$.

5.3 Proprioceptive Sensors

The adoption of *sensors* is of crucial importance to achieve high-performance robotic systems. It is worth classifying sensors into *proprioceptive* sensors that measure the internal state of the manipulator, and *exteroceptive* sensors that provide the robot with knowledge of the surrounding environment.

In order to guarantee that a coordinated motion of the mechanical structure is obtained in correspondence of the task planning, suitable parameter identification and control algorithms are used which require the on-line measurement, by means of proprioceptive sensors, of the quantities characterizing the internal state of the manipulator, i.e.:

- joint positions,
- joint velocities,
- joint torques.

On the other hand, typical exteroceptive sensors include:

- force sensors,
- tactile sensors,
- proximity sensors,
- range sensors,
- vision sensors.

The goal of such sensors is to extract the features characterizing the interaction of the robot with the objects in the environment, so as to enhance the degree of autonomy of the system. To this class also belong those sensors which are specific for the robotic application, such as sound, humidity, smoke, pressure, and temperature sensors. Fusion of the available sensory data can be used for (high-level) task planning, which in turn characterizes a *robot* as the *intelligent connection of perception to action*.

In the following, the main features of the proprioceptive sensors are illustrated, while those of the exteroceptive sensors will be presented in the next section.

5.3.1 Position Transducers

The aim of *position transducers* is to provide an electric signal proportional to the linear or angular displacement of a mechanical apparatus with respect to a given reference position. They are mostly utilized for control of machine tools, and thus their range is wide. Potentiometers, linear variable-differential transformers (LVDT), and inductosyns may be used to measure linear displacements. Potentiometers, encoders, resolvers and synchros may be used to measure angular displacements.

Angular displacement transducers are typically employed in robotics applications since, also for prismatic joints, the servomotor is of a rotary type. In view of their precision, robustness and reliability, the most common transducers are the *encoders* and *resolvers*, whose operating principles are detailed in what follows.

On the other hand, linear displacement transducers (LVDT's and inductosyns) are mainly employed in measuring robots.

Encoder

There are two types of encoder: absolute and incremental. The *absolute encoder* consists of an optical-glass disk on which concentric circles (tracks) are disposed; each track has an alternating sequence of transparent sectors and matte sectors obtained by deposit of a metallic film. A light beam is emitted in

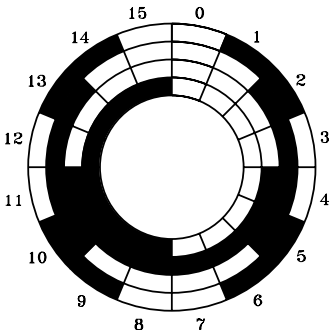

Fig. 5.12. Schematic representation of an absolute encoder

correspondence of each track which is intercepted by a photodiode or a phototransistor located on the opposite side of the disk. By a suitable arrangement of the transparent and matte sectors, it is possible to convert a finite number of angular positions into corresponding digital data. The number of tracks determines the length of the word, and thus the resolution of the encoder.

To avoid problems of incorrect measurement in correspondence of a simultaneous multiple transition between matte and transparent sectors, it is worth utilizing a Gray-code encoder whose schematic representation is given in Fig. 5.12 with reference to the implementation of 4 tracks that allow the discrimination of 16 angular positions. It can be noticed that measurement ambiguity is eliminated, since only one change of contrast occurs at each transition (Table 5.1). For the typical resolution required for joint control, absolute encoders with a minimum number of 12 tracks (bits) are employed (resolution of 1/4096 per circle). Such encoders can provide unambiguous measurements only in a circle. If a gear reduction is present, a circle at the joint side corresponds to several circles at the motor side, and thus a simple electronics is needed to count and store the number of actual circles.

Table 5.1. Coding table with Gray-code

#	Code	#	Code
0	0000	8	1100
1	0001	9	1101
2	0011	10	1111
3	0010	11	1110
4	0110	12	1010
5	0111	13	1011
6	0101	14	1001
7	0100	15	1000

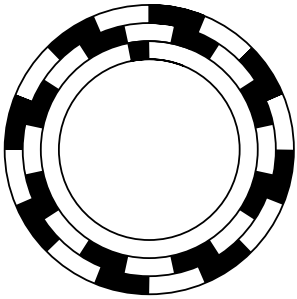

Fig. 5.13. Schematic representation of an incremental encoder

Incremental encoders have a wider use than absolute encoders, since they are simpler from a construction viewpoint and thus cheaper. Like the absolute one, the incremental encoder consists of an optical disk on which two tracks are disposed, whose transparent and matte sectors (in equal number on the two tracks) are mutually in quadrature. The presence of two tracks also allows, besides the number of transitions associated with any angular rotation, the detection of the sign of rotation. Often a third track is present with one single matte sector which allows the definition of an absolute mechanical zero as a reference for angular position. A schematic representation is illustrated in Fig. 5.13.

The use of an incremental encoder for a joint actuating system clearly demands the evaluation of absolute positions. This is performed by means of suitable counting and storing electronic circuits. To this end, it is worth noticing that the position information is available on volatile memories, and thus it can be corrupted due to the effect of disturbances acting on the electronic circuit, or else fluctuations in the supply voltage. Such limitation obviously does not occur for absolute encoders, since the angular position information is coded directly on the optical disk.

The optical encoder has its own signal processing electronics inside the case, which provides direct digital position measurements to be interfaced with the control computer. If an external circuitry is employed, velocity measurements can be reconstructed from position measurements. In fact, if a pulse is generated at each transition, a velocity measurement can be obtained in three possible ways, namely, by using a voltage-to-frequency converter (with analog output), by (digitally) measuring the frequency of the pulse train, or by (digitally) measuring the sampling time of the pulse train. Between these last two techniques, the former is suitable for high-speed measurements while the latter is suitable for low-speed measurements.

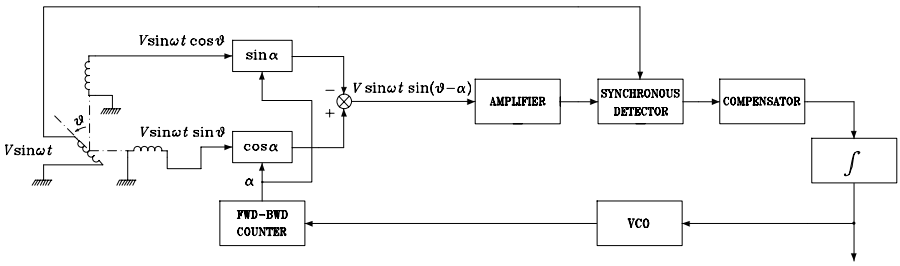

Fig. 5.14. Electric scheme of a resolver with functional diagram of a tracking-type RDC

Resolver

The resolver is an electromechanical position transducer which is compact and robust. Its operating principle is based on the mutual induction between two electric circuits which allow continuous transmission of angular position without mechanical limits. The information on the angular position is associated with the magnitude of two sinusoidal voltages, which are treated by a suitable resolver-to-digital converter (RDC) to obtain the digital data corresponding to the position measurement. The electric scheme of a resolver with the functional diagram of a tracking-type RDC is illustrated in Fig. 5.14.

From a construction viewpoint, the resolver is a small electric machine with a rotor and a stator; the inductance coil is on the rotor while the stator has two windings at 90 electrical degrees one from the other. By feeding the rotor with a sinusoidal voltage $V \sin \omega t$ (with typical frequencies in the range of 0.4 to 10 kHz), a voltage is induced on the stator windings whose magnitude depends on the rotation angle θ. The two voltages are fed to two digital multipliers, whose input is α and whose outputs are algebraically summed to achieve $V \sin \omega t \sin(\theta - \alpha)$; this signal is then amplified and sent to the input of a synchronous detector, whose filtered output is proportional to the quantity $\sin(\theta - \alpha)$. The resulting signal, after a suitable compensating action, is integrated and then sent to the input of a voltage-controlled oscillator (VCO) (a voltage-to-frequency converter) whose output pulses are input to a forward-backward counter. Digital data of the quantity α are available on the output register of the counter, which represent a measurement of the angle θ.

It can be recognized that the converter works according to a feedback principle. The presence of two integrators (one is represented by the forward-backward counter) in the loop ensures that the (digital) position and (analog) velocity measurements are error-free as long as the rotor rotates at constant speed; actually, a round-off error occurs on the word α and thus affects the position measurement. The compensating action is needed to confer suitable stability properties and bandwidth to the system. Whenever digital data are wished also for velocity measurements, it is necessary to use an analog-to-

digital converter. Since the resolver is a very precise transducer, a resolution of 1 bit out of 16 can be obtained at the output of the RDC.

5.3.2 Velocity Transducers

Even though velocity measurements can be reconstructed from position transducers, it is often preferred to resort to direct measurements of velocity, by means of suitable transducers. *Velocity transducers* are employed in a wide number of applications and are termed *tachometers*. The most common devices of this kind are based on the operating principles of electric machines. The two basic types of tachometers are the *direct-current (DC) tachometer* and the *alternating-current (AC) tachometer*.

DC tachometer

The direct-current tachometer is the most used transducer in the applications. It is a small DC generator whose magnetic field is provided by a permanent magnet. Special care is paid to its construction, so as to achieve a linear input/output relationship and to reduce the effects of magnetic hysteresis and temperature. Since the field flux is constant, when the rotor is set in rotation, its output voltage is proportional to angular speed according to the constant characteristic of the machine.

Because of the presence of a commutator, the output voltage has a residual ripple which cannot be eliminated by proper filtering, since its frequency depends on angular speed. A linearity range of 0.1 to 1% can be obtained, whereas the residual ripple coefficient is of 2 to 5% of the mean value of the output signal.

AC tachometer

In order to avoid the drawbacks caused by the presence of a residual ripple in the output of a DC tachometer, one may resort to an AC tachometer. While the DC tachometer is a true DC generator, the AC tachometer differs from a generator. In fact, if a synchronous generator would be used, the frequency of the output signal would be proportional to the angular speed.

To obtain an alternating voltage whose magnitude is proportional to speed, one may resort to an electric machine that is structurally different from the synchronous generator. The AC tachometer has two windings on the stator mutually in quadrature and a cup rotor. If one of the windings is fed by a constant-magnitude sinusoidal voltage, a sinusoidal voltage is induced on the other winding which has the same frequency, a magnitude proportional to angular speed, and a phase equal or opposite to that of the input voltage according to the sign of rotation; the exciting frequency is usually set to 400 Hz. The use of a synchronous detector then yields an analog measurement

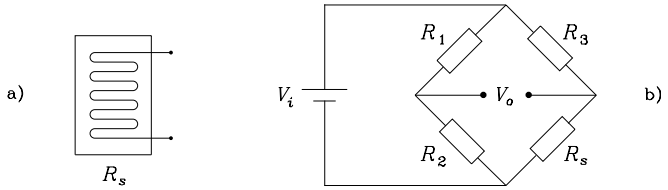

Fig. 5.15. a) Schematic representation of a strain gauge. **b)** Its insertion in a Wheatstone bridge

of angular velocity. In this case, the output ripple can be eliminated by a proper filter, since its fundamental frequency is twice as much as the supply frequency.

The performance of AC tachometers is comparable to that of DC tachometers. Two further advantages of AC tachometers are the lack of wiping contacts and the presence of a low moment of inertia, in view of the use of a lightweight cup rotor. However, a residual voltage occurs, even when the rotor is still, because of the unavoidable parasitic couplings between the stator coil and the measurement circuitry.

5.4 Exteroceptive Sensors

5.4.1 Force Sensors

Measurement of a force or torque is usually reduced to measurement of the strain induced by the force (torque) applied to an extensible element of suitable features. Therefore, an indirect measurement of force is obtained by means of measurements of small displacements. The basic component of a force sensor is the *strain gauge* which uses the change of electric resistance of a wire under strain.

Strain gauge

The strain gauge consists of a wire of low temperature coefficient. The wire is disposed on an insulated support (Fig. 5.15a) which is glued to the element subject to strain under the action of a stress. Dimensions of the wire change and then they cause a change of electric resistance.

The strain gauge is chosen in such a way that the resistance R_s changes linearly in the range of admissible strain for the extensible element. To transform changes of resistance into an electric signal, the strain gauge is inserted in one arm of a Wheatstone bridge which is balanced in the absence of stress on the strain gauge itself. From Fig. 5.15b it can be understood that the voltage balance in the bridge is described by

$$V_o = \left(\frac{R_2}{R_1 + R_2} - \frac{R_s}{R_3 + R_s} \right) V_i. \tag{5.30}$$

If temperature variations occur, the wire changes its dimension without application of any external stress. To reduce the effect of temperature variations on the measurement output, it is worth inserting another strain gauge in an adjacent arm of the bridge, which is glued on a portion of the extensible element not subject to strain.

Finally, to increase bridge sensitivity, two strain gauges may be used which have to be glued on the extensible element in such a way that one strain gauge is subject to traction and the other to compression; the two strain gauges then have to be inserted in two adjacent arms of the bridge.

Shaft torque sensor

In order to employ a servomotor as a torque-controlled generator, an indirect measurement of the driving torque is typically used, e.g., through the measurement of armature current in a permanent-magnet DC servomotor. If it is desired to guarantee insensitivity to change of parameters relating torque to the measured physical quantities, it is necessary to resort to a direct torque measurement.

The torque delivered by the servomotor to the joint can be measured by strain gauges mounted on an extensible apparatus interposed between the motor and the joint, e.g., a hollow shafting. Such apparatus must have low torsional stiffness and high bending stiffness, and it must ensure a proportional relationship between the applied torque and the induced strain.

By connecting the strain gauges mounted on the hollow shafting (in a Wheatstone bridge configuration) to a slip ring by means of graphite brushes, it is possible to feed the bridge and measure the resulting unbalanced signal which is proportional to the applied torque.

The measured torque is that delivered by the servomotor to the joint, and thus it does not coincide with the driving torque C_m in the block schemes of the actuating systems in Fig. 5.2 and in Fig. 5.6. In fact, such measurement does not account for the inertial and friction torque contributions as well as for the transmission located upstream of the measurement point.

Wrist force sensor

When the manipulator's end-effector is in contact with the working environment, the *force sensor* allows the measurement of the three components of a force and the three components of a moment with respect to a frame attached to it.

As illustrated in Fig. 5.16, the sensor is employed as a connecting apparatus at the wrist between the outer link of the manipulator and the end-effector. The connection is made by means of a suitable number of extensible elements subject to strain under the action of a force and a moment. Strain gauges are glued on each element which provide strain measurements. The elements

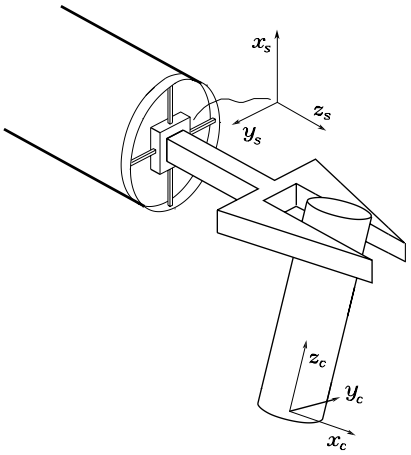

Fig. 5.16. Use of a force sensor on the outer link of a manipulator

have to be disposed in a keen way so that at least one element is appreciably deformed for any possible orientation of forces and moments.

Furthermore, the single force component with respect to the frame attached to the sensor should induce the least possible number of deformations, so as to obtain good structural decoupling of force components. Since a complete decoupling cannot be achieved, the number of significant deformations to reconstruct the six components of the force and moment vector is greater than six.

A typical force sensor is that where the extensible elements are disposed as in a Maltese cross; this is schematically indicated in Fig. 5.17. The elements connecting the outer link with the end-effector are four bars with a rectangular parallelepiped shape. On the opposite sides of each bar, a pair of strain gauges is glued that constitute two arms of a Wheatstone bridge; there is a total of eight bridges and thus the possibility of measuring eight strains.

The matrix relating strain measurements to the force components expressed in a Frame s attached to the sensor is termed sensor *calibration matrix*. Let w_i, for $i = 1, \ldots, 8$, denote the outputs of the eight bridges providing measurement of the strains induced by the applied forces on the bars according

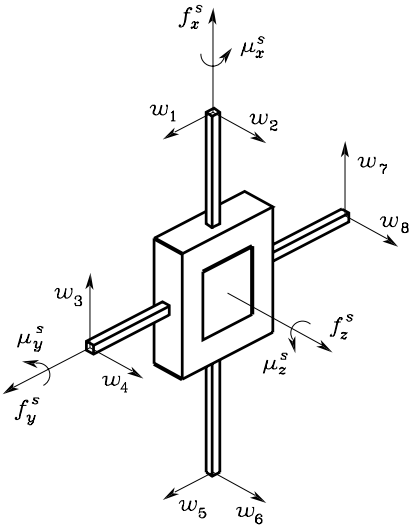

Fig. 5.17. Schematic representation of a Maltese-cross force sensor

to the directions specified in Fig. 5.17. Then, the calibration matrix is given by the transformation

$$\begin{bmatrix} f_x^s \\ f_y^s \\ f_z^s \\ \mu_x^s \\ \mu_y^s \\ \mu_z^s \end{bmatrix} = \begin{bmatrix} 0 & 0 & c_{13} & 0 & 0 & 0 & c_{17} & 0 \\ c_{21} & 0 & 0 & 0 & c_{25} & 0 & 0 & 0 \\ 0 & c_{32} & 0 & c_{34} & 0 & c_{36} & 0 & c_{38} \\ 0 & 0 & 0 & c_{44} & 0 & 0 & 0 & c_{48} \\ 0 & c_{52} & 0 & 0 & 0 & c_{56} & 0 & 0 \\ c_{61} & 0 & c_{63} & 0 & c_{65} & 0 & c_{67} & 0 \end{bmatrix} \begin{bmatrix} w_1 \\ w_2 \\ w_3 \\ w_4 \\ w_5 \\ w_6 \\ w_7 \\ w_8 \end{bmatrix} . \tag{5.31}$$

Reconstruction of force measurements through the calibration matrix is entrusted to suitable signal processing circuitry available in the sensor.

Typical sensors have a diameter of about 10 cm and a height of about 5 cm, with a measurement range of 50 to 500 N for the forces and of 5 to 70 N·m for the torques, and a resolution of the order of 0.1% of the maximum force and of 0.05% of the maximum torque, respectively; the sampling frequency at the output of the processing circuitry is of the order of 1 kHz.

Finally, it is worth noticing that force sensor measurements cannot be directly used by a force/motion control algorithm, since they describe the equivalent forces acting on the sensors which differ from the forces applied to the manipulator's end-effector (Fig. 5.16). It is therefore necessary to trans-

form those forces from the sensor Frame s into the constraint Frame c; in view of the transformation in (3.116), one has

$$\begin{bmatrix} \boldsymbol{f}_c^c \\ \boldsymbol{\mu}_c^c \end{bmatrix} = \begin{bmatrix} \boldsymbol{R}_s^c & \boldsymbol{O} \\ \boldsymbol{S}(\boldsymbol{r}_{cs}^c)\boldsymbol{R}_s^c & \boldsymbol{R}_s^c \end{bmatrix} \begin{bmatrix} \boldsymbol{f}_s^s \\ \boldsymbol{\mu}_s^s \end{bmatrix} \tag{5.32}$$

which requires knowledge of the position $\boldsymbol{r}_{cs}^c$ of the origin of Frame s with respect to Frame c as well as of the orientation $\boldsymbol{R}_s^c$ of Frame s with respect to Frame c. Both such quantities are expressed in Frame c, and thus they are constant only if the end-effector is still, once contact has been achieved.

5.4.2 Range Sensors

The primary function of the exteroceptive sensors is to provide the robot with the information needed to execute 'intelligent' actions in an autonomous way. To this end, it is crucial to detect the presence of an object in the workspace and eventually to measure its range from the robot along a given direction.

The former kind of data is provided by the *proximity sensors*, a simplified type of *range sensors*, capable of detecting only the presence of objects nearby the sensitive part of the sensor, without a physical contact. The distance within which such sensors detect objects is defined *sensitive range*.

In the more general case, range sensors are capable of providing structured data, given by the distance of the measured object and the corresponding measurement direction, i.e., the position in space of the detected object with respect to the sensor.

The data provided by the range sensors are used in robotics to avoid obstacles, build maps of the environment, recognize objects.

The most popular range sensors in robotics applications are those based on sound propagation through an elastic fluid, the so-called *sonars* (SOund NAvigation and Ranging), and those exploiting light propagation features, the so-called *lasers* (Light Amplification by Stimulated Emission of Radiation). In the following, the main features of these two sensors are illustrated.

Sonars

The sonars employ acoustic pulses and their echoes to measure the range to an object. Since the sound speed is usually known for a given media (air, water), the range to an object is proportional to the echo travel time, commonly called *time-of-flight*, i.e., the time which the acoustic wave takes to cover the distance sensor-object-sensor. Sonars are widely utilized in robotics, and especially in mobile and underwater robotics. Their popularity is due to their low cost, light weight, low power consumption, and low computational effort, compared to other ranging sensors. In some applications, such as in underwater and low-visibility environments, the sonar is often the only viable sensing modality.

Despite a few rare examples of sonars operating at audible frequencies for human ears (about 20 Hz to 20 KHz), the ultrasound frequencies (higher

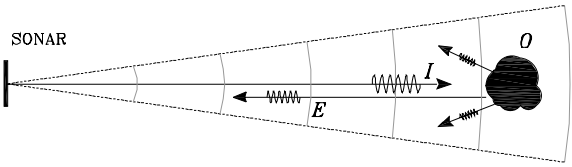

Fig. 5.18. Sonar ranging principle

than 20 KHz) are the most widely used to realize this type of sensor. Typical frequencies in robotics range from 20 KHz to 200 KHz, even though higher values (of the order of MHz) can be achieved utilizing piezoelectric quartz crystals. In this range, the energy of the wave emitted by the sonar can be regarded as concentrated in a conical volume whose beamwidth depends on the frequency as well as on the transducer diameter. Further to measuring range, sonars provide qualitative directional data on the object which has generated the echo. For the most common sensors in robotics, the beamwidth of the energy beam is typically not smaller than 15 deg. Obviously, for smaller beamwidths, higher angular resolutions can be obtained.

The main components of a sonar measurement system are a transducer, which is vibrated and transforms acoustic energy into electric energy and vice versa, and a circuitry for the excitation of the transducer and the detection of the reflected signal. Figure 5.18 schematically illustrates the operating principle: the pulse I emitted by the transducer, after hitting the object O found in the emission cone of the sensor, is partly reflected (echo E) towards the sound source and thus detected. The time-of-flight t_v is the time between the emission of the ultrasound pulse and the reception of the echo. The object range d_O can be computed from t_v using the relation

$$d_O = \frac{c_s t_v}{2} \tag{5.33}$$

where c_s is sound speed, which in low-humidity air depends on the temperature T (measured in centigrade) according to the expression

$$c_s \approx 20.05\sqrt{T + 273.16} \text{ m/s}. \tag{5.34}$$

In the scheme of Fig. 5.18 the use of a sole transducer is represented for the transmission of the pulse and the reception of the echo. This configuration requires that the commutation from transmitter to receiver takes place after a certain latency time which depends not only on the duration of the transmitted pulse but also on the mechanical inertia of the transducer.

Despite the low cost and ease of use, however, these sensors have non-negligible limits with respect to the angular and radial resolution, as well as to the minimum and maximum measurement range that can be achieved. In particular, the width of the radiation cone decreases as frequency increases with improved angular resolution. A higher frequency leads to greater radial

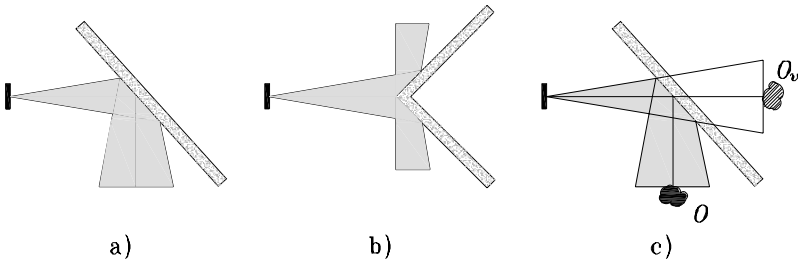

Fig. 5.19. Reflector models on smooth surfaces: **a)** non-detected plane. **b)** non-detected corner. **c)** plane with false detection (O real object, O_v virtual object detected)

resolution and contributes to reducing the minimum range that can be detected by the sonar. Nevertheless, there is a lower limit because of the lapse time when reception is inhibited to avoid interference with the reflected signal — in certain cases better performance can be obtained by employing two distinct transducers for the emission and the detection. On the other hand, too high frequencies may exasperate absorbtion phenomena, depending on the features of the surface generating the echo. Such phenomena further reduce the power of the transmitted signal — decreasing with the square of the range covered by the ultrasound wave — thus reducing the maximum limit of the measurement time.

Piezoelectric and electrostatic transducers are the two major types available that operate in air and can in principle operate both as a transmitter and receiver.

The *piezoelectric transducers* exploit the property of some crystal materials to deform under the action of an electric field and vibrate when a voltage is applied at the resonant frequency of the crystal. The efficiency of the acoustic match of these transducers with compressible fluids such as air is rather low. Often a conical concave horn is mounted on the crystal to match acoustically the crystal acoustic impedance to that of air. Being of resonant type, these transducers are characterized by a rather low bandwidth and show a significant mechanical inertia which severely limits the minimum detectable range, thus justifying the use of two distinct transducers as transmitter and receiver.

The *electrostatic transducers* operate as capacitors whose capacitance varies moving and/or deforming one of its plates. A typical construction consists of a gold-coated plastic foil membrane (*mobile* plate) stretched across a round grooved aluminium back plate (*fixed* plate). When the transducer operates as receiver, the change of capacitance, induced by the deformation of the membrane under the acoustic pressure, produces a proportional change of the voltage across the capacitor, assuming that the foil charge is constant. As a transmitter, the transducer membrane is vibrated by applying a sequence of electric pulses across the capacitor. The electric oscillations generate, as

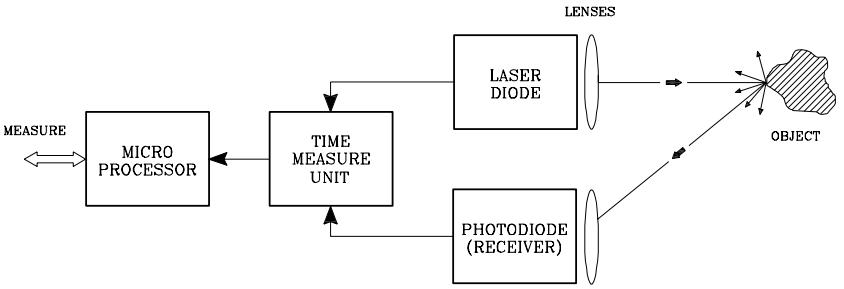

Fig. 5.20. Time-of-flight laser sensor operating principle

a result of the induced electric field, a mechanical force which vibrates the mobile plate.

Since the electrostatic transducers can operate at different frequencies, they are characterized by large bandwidth and high sensitivity, low mechanical inertia and rather efficient acoustic match with air. As compared to the piezoelectric transducers, however, they can operate at lower maximum frequencies (a few hundreds kHz vs a few MHz) and require a bias voltage which complicates the control electronics. Among the ultrasound measurement systems with capacitive transducers, it is worth mentioning the Polaroid sonar, initially developed for autofocus systems and later widely employed as range sensors in several robotic applications. The 600 series sensor utilizes a capacitive transducer of the type described above with a diameter of almost 4 cm, operates at 50 kHz frequency and is characterized by a beamwidth of 15 deg, can detect a maximum range of about 10 m and a mimimum range of about 15 cm with an accuracy of $\pm 1\%$ across the measurement range. The bias voltage is 200 V with current absorbtion peaks of 2 A in transmission.

Accuracy of ultrasound range sensors depends on the features of the transducer and the excitation/detection circuitry, as well as on the reflective properties of the surfaces hit by the acoustic waves.

Smooth surfaces, i.e., those characterized by irregularities of comparable size to that of the wavelength corresponding to the employed frequency, may produce a non-detectable echo at the sensor (Figura 5.19a,b) if the incident angle of the ultrasound beam exceeds a given critical angle which depends on the operational frequency and the reflective material. In the case of the Polaroid sensors, this angle is equal to 65 deg, i.e., 25 deg from the normal to the reflective surface, for a smooth surface in plywood. When operating in complex environments, such mirror reflections may give rise to multiple reflections, thus causing range measurement errors or false detection (Fig. 5.19c).

Lasers

In the construction of optical measurement systems, the laser beam is usually preferred to other light sources for the following reasons:

- They can easily generate bright beams with lightweight sources.
- The infrared beams can be used unobtrusively.
- They focus well to give narrow beams.
- Single-frequency sources allow easier rejection filtering of unwanted frequencies, and do not disperse from refraction as much as full spectrum sources.

There are two types of laser-based range sensors in common use: the time-of-flight sensors and the triangulation sensors.

The *time-of-flight sensors* compute distance by measuring the time that a pulse of light takes to travel from the source to the observed target and then to the detector (usually collocated with the source). The travel time multiplied by the speed of light (properly adjusted for the air temperature) gives the distance measurement. The operating principle of a time-of-flight laser sensor is illustrated in Fig. 5.20.

Limitations on the accuracy of these sensors are based on the minimum observation time — and thus the minimum distance observable, the temporal accuracy (or quantization) of the receiver, and the temporal width of the laser pulse. Such limitations are not only of a technological nature. In many cases, cost is the limiting factor of these measurement devices. For instance, to obtain 1 mm resolution, a time accuracy of about 3 ps, which can be achieved only by using rather expensive technology.

Many time-of-flight sensors used have what is called an *ambiguity interval*. The sensor emits pulses of light periodically, and computes an average target distance from the time of the returning pulses. Typically, to simplify the detection electronics of these sensors, the receiver only accepts signals that arrive within time Δt, but this time window might also observe previous pulses reflected by more distant surfaces. This means that a measurement is ambiguous to the multiple of $\frac{1}{2}c\Delta t$, where c is the speed of light. Typical values of $\frac{1}{2}c\Delta t$ are 20–40 m.

In certain conditions, suitable algorithms can be employed to recover the true depth by assuming that the distances should be changing smoothly.

The time-of-flight sensors transmit only a single beam, thus range measurements are only obtained from a single surface point. In order to obtain more information, the range data is usually supplied as a vector of range to surfaces lying in a plane or as an image. To obtain these denser representations, the laser beam is swept across the scene. Normally the beam is swept by a set of mirrors rather than moving the laser and detector themselves — mirrors are lighter and less prone to motion damage.

Typical time-of-flight sensors suitable for mobile robotics applications have a range of 5–100 m, an accuracy of 5–10 mm, and a frequency of data acquisition per second of 1000–25000 Hz.

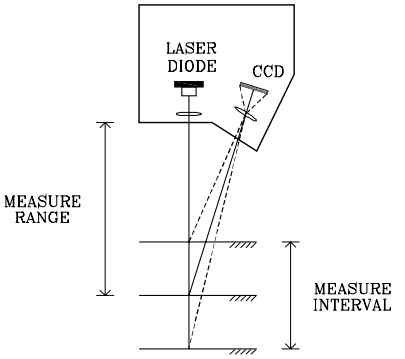

Fig. 5.21. Triangulation laser sensor operating principle

The operating principle of *triangulation laser sensors*[3] is illustrated in Fig. 5.21.

The laser beam emitted by a photodiode is projected onto the observed surface. The reflected beam is focused on a CCD sensor by means of a suitable lens. Obviously, reflection must be diffused. The position of the focused beam reflected to the receiver gives rise to a signal which is proportional to the distance of the transmitter from the object. In fact, from the measurement of the CCD sensor it is possible to resort to the angle at which the reflected energy hits the sensor. Once the relative position and orientation of the CCD sensor with respect to the photodiode are known, as e.g. through a suitable calibration procedure, it is possible to compute the distance from the object with simple geometry.

Accuracy can be influenced by certain object surfaces not favouring reflection, differences or changes of colour. Such occurrences can be mitigated or even eliminated with modern electronic technology and automatic regulation of light intensity.

The possibility of controlling the laser beam light brings the following advantages:

[3] The triangulation method is based on the trigonometric properties of triangles and in particular on the cosine theorem. The method allows the computation of the distance between two non-directly accessible points, i.e., once two angles and one side of a triangle are known, it is possible to determine the other two sides. For the case at issue, one side is given by the distance between the emitter (laser) and the receiver (the CCD sensor), one angle is given by the orientation of the emitter with respect to that side and the other angle can be computed from the position of the laser beam on the image plane. In practice, it is not easy to compute the above quantities, and suitable calibration techniques are to be employed which avoid such computation to determine the distance measurement.

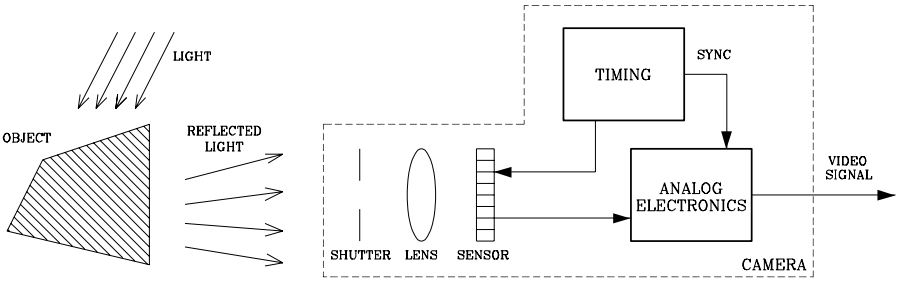

Fig. 5.22. Schematic representation of a vision system

- If the laser beam wavelength is known, e.g. that of the visible red 670 nm, highly selective filters can be used which are set to the same frequency to reduce the effects of other light sources.
- The laser beam may be remodelled through lenses and mirrors so as to create multiple beams or laser strips to measure multiple 3D points simultaneously.
- The direction of the laser beam can be controlled directly by the control system to observe selectively only those portions of the scene of interest.

The main limitations of this type of sensors are the potential eye safety risks from the power of lasers, particularly when invisible laser frequencies are used (commonly infrared), as well as the false specular reflections from metallic and polished objects.

5.4.3 Vision Sensors

The task of a camera as a *vision sensor* is to measure the intensity of the light reflected by an object. To this end, a photosensitive element, termed *pixel* (or *photosite*), is employed, which is capable of transforming light energy into electric energy. Different types of sensors are available depending on the physical principle exploited to realize the energy transformation. The most widely used devices are CCD and CMOS sensors based on the photoelectric effect of semiconductors.

CCD

A CCD (Charge Coupled Device) sensor consists of a rectangular array of photosites. Due to the photoelectric effect, when a photon hits the semiconductor surface, a number of free electrons are created, so that each element accumulates a charge depending on the time integral of the incident illumination over the photosensitive element. This charge is then passed by a transport mechanism (similar to an analog shift register) to the output amplifier, while at

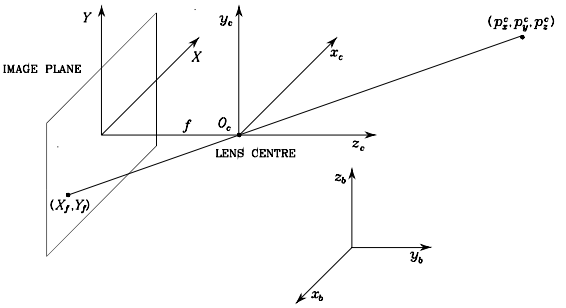

Fig. 5.23. Perspective transformation

the same time the photosite is discharged. The electric signal is to be further processed in order to produce the real *video signal*.

CMOS

A CMOS (Complementary Metal Oxide Semiconductor) sensor consists of a rectangular array of photodiodes. The junction of each photodiode is precharged and it is discharged when hit by photons. An amplifier integrated in each pixel can transform this charge into a voltage or current level. The main difference with the CCD sensor is that the pixels of a CMOS sensor are non-integrating devices; after being activated they measure throughput, not volume. In this manner, a saturated pixel will never overflow and influence a neighboring pixel. This prevents the effect of *blooming*, which indeed affects CCD sensors.

Camera

As sketched in Fig. 5.22, a camera is a complex system comprising several devices other than the photosensitive sensor, i.e., a *shutter*, a *lens* and *analog preprocessing electronics*. The lens is responsible for focusing the light reflected by the object on the plane where the photosensitive sensor lies, called the *image plane*.

With reference to Fig. 5.23, consider a frame O_c–$x_c y_c z_c$ attached to the camera, whose location with respect to the base frame is identified by the homogeneous transformation matrix $\boldsymbol{T}_c^b$. Take a point of the object of coordinates $\boldsymbol{p}^c = [\, p_x^c \quad p_y^c \quad p_z^c \,]^T$; typically, the centroid of the object is chosen. Then, the coordinate transformation from the base frame to the camera frame is described as

$$\widetilde{\boldsymbol{p}}^c = \boldsymbol{T}_b^c \widetilde{\boldsymbol{p}}, \tag{5.35}$$

where $\boldsymbol{p}$ denotes the object position with respect to the base frame and homogeneous representations of vectors have been used.

A reference frame can be introduced on the image plane, whose axes X and Y are parallel to the axes x_c and y_c of the camera frame, and the origin is at the intersection of the optical axis with the image plane, termed principal point. Due to the refraction phenomenon, the point in the camera frame is transformed into a point in the image plane via the *perspective transformation*, i.e.,

$$X_f = -\frac{f p_x^c}{p_z^c}$$
$$Y_f = -\frac{f p_y^c}{p_z^c}$$

where (X_f, Y_f) are the new coordinates in the frame defined on the image plane, and f is the *focal length* of the lens. Notice that these coordinates are expressed in metric units and the above transformation is singular at $p_z^c = 0$.

The presence of the minus sign in the equations of the perspective transformation is consistent with the fact that the image of an object appears upside down on the image plane of the camera. Such an effect can be avoided, for computational ease, by considering a virtual image plane positioned before the lens, in correspondence of the plane $z_c = f$ of the camera frame. In this way, the model represented in Fig. 5.24 is obtained, which is characterized by the *frontal* perspective transformation

$$X_f = \frac{f p_x^c}{p_z^c} \tag{5.36}$$
$$Y_f = \frac{f p_y^c}{p_z^c} \tag{5.37}$$

where, with abuse of notation, the name of the variables on the virtual plane has not been changed.

These relationships hold only in theory, since the real lenses are always affected by imperfections, which cause image quality degradation. Two types of distortions can be recognized, namely, *aberrations* and *geometric distortion*. The former can be reduced by restricting the light rays to a small central region of the lens; the effects of the latter can be compensated on the basis of a suitable model whose parameters are to be identified.

A visual information is typically elaborated by a digital processor, and thus the measurement principle is to transform the light intensity $I(X, Y)$ of each point in the image plane into a number. It is clear that a *spatial sampling* is needed since an infinite number of points in the image plane exist, as well as a *temporal sampling* since the image can change during time. The CCD or CMOS sensors play the role of spatial samplers, while the shutter in front of the lens plays the role of the temporal sampler.

The spatial sampling unit is the pixel, and thus the coordinates (X, Y) of a point in the image plane are to be expressed in pixels, i.e., (X_I, Y_I). Due to the

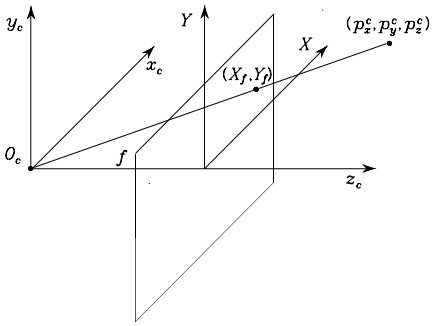

Fig. 5.24. Frontal perspective transformation

photosite finite dimensions, the pixel coordinates of the point are related to the coordinates in metric units through two scale factors α_x and α_y, namely,

$$X_I = \frac{\alpha_x f p_x^c}{p_z^c} + X_0 \tag{5.38}$$

$$Y_I = \frac{\alpha_y f p_y^c}{p_z^c} + Y_0, \tag{5.39}$$

where X_0 and Y_0 are the offsets which take into account the position of the origin of the pixel coordinate system with respect to the optical axis. This nonlinear transformation can be written in a linear form by resorting to the homogeneous representation of the point (x_I, y_I, z_I) via the relationships

$$X_I = \frac{x_I}{\lambda}$$
$$Y_I = \frac{y_I}{\lambda}$$

where $\lambda > 0$. As a consequence, (5.38), (5.39) can be rewritten as

$$\begin{bmatrix} x_I \\ y_I \\ \lambda \end{bmatrix} = \lambda \begin{bmatrix} X_I \\ Y_I \\ 1 \end{bmatrix} = \boldsymbol{\Omega\Pi} \begin{bmatrix} p_x^c \\ p_y^c \\ p_z^c \\ 1 \end{bmatrix} \tag{5.40}$$

where

$$\boldsymbol{\Omega} = \begin{bmatrix} f\alpha_x & 0 & X_0 \\ 0 & f\alpha_y & Y_0 \\ 0 & 0 & 1 \end{bmatrix} \tag{5.41}$$

$$\boldsymbol{\Pi} = \begin{bmatrix} 1 & 0 & 0 & 0 \\ 0 & 1 & 0 & 0 \\ 0 & 0 & 1 & 0 \end{bmatrix}. \tag{5.42}$$

At this point, the overall transformation from the Cartesian space of the observed object to the *image space* of its image in pixels is characterized by composing the transformations in (5.35), (5.40) as

$$\Xi = \boldsymbol{\Omega \Pi T}_b^c \tag{5.43}$$

which represents the so-called *camera calibration* matrix. It is worth pointing out that such a matrix contains *intrinsic parameters* $(\alpha_x, \alpha_y, X_0, Y_0, f)$ in $\boldsymbol{\Omega}$ depending on the sensor and lens characteristics as well as *extrinsic parameters* in $\boldsymbol{T}_c^b$ depending on the relative position and orientation of the camera with respect to the base frame. Several calibration techniques exist to identify these parameters in order to compute the transformation between the Cartesian space and the image space as accurately as possible.

If the intrinsic parameters of a camera are known, from a computationally viewpoint, it is convenient to refer to the *normalized coordinates* (X, Y), defined by the normalized perspective transformation

$$\lambda \begin{bmatrix} X \\ Y \\ 1 \end{bmatrix} = \boldsymbol{\Pi} \begin{bmatrix} p_x^c \\ p_y^c \\ p_z^c \\ 1 \end{bmatrix}. \tag{5.44}$$

These coordinates are defined in metrical units and coincide with the coordinates (5.36), (5.37) in the case when $f = 1$. Comparing (5.40) with (5.44) yields the invertible transformation

$$\begin{bmatrix} X_I \\ Y_I \\ 1 \end{bmatrix} = \boldsymbol{\Omega} \begin{bmatrix} X \\ Y \\ 1 \end{bmatrix} \tag{5.45}$$

relating the normalized coordinates to those expressed in pixels through the matrix of intrinsic parameters.

If a monochrome CCD camera[4] is of concern, the output amplifier of the sensor produces a signal which is processed by a timing analog electronics in order to generate an electric signal according to one of the existing *video standards*, i.e., the CCIR European and Australian standard, or the RS170 American and Japanese standard. In any case, the video signal is a voltage of 1 V peak-to-peak whose amplitude represents sequentially the image intensity.

The entire image is divided into a number of lines (625 for the CCIR standard and 525 for the RS170 standard) to be sequentially scanned. The raster scan proceeds horizontally across each line and each line from top to bottom, but first all the even lines, forming the first *field*, and then all the odd lines, forming the second *field*, so that a *frame* is composed of two successive

[4] Colour cameras are equipped with special CCDs sensitive to three basic colours (RGB); the most sophisticated cameras have three separate sensors, one per each basic colour.

fields. This technique, called *interlacing*, allows the image to be updated either at frame rate or at field rate; in the former case the update frequency is that of the entire frame (25 Hz for the CCIR standard and 30 Hz for the RS170 standard), while in the latter case the update frequency can be doubled as long as half the vertical resolution can be tolerated.

The last step of the measurement process is to digitize the analog video signal. The special analog-to-digital converters adopted for video signal acquisition are called *frame grabbers*. By connecting the output of the camera to the frame grabber, the video waveform is sampled and quantized and the values stored in a two-dimensional memory array representing the spatial sample of the image, known as *framestore*; this array is then updated at field or frame rate.

In the case of CMOS cameras (currently available only for monochrome images), thanks to CMOS technology which allows the integration of the analog-to-digital converter in each pixel, the output of the camera is directly a two-dimensional array, whose elements can be accessed randomly. Such advantage, with respect to CCD cameras, leads to the possibility of higher frame rates if only parts of the entire frame are accessed.

The sequence of steps from image formation to image acquisition described above can be classified as a process of *low-level vision*; this includes the extraction of elementary image features, e.g., centroid and intensity discontinuities. On the other hand, a robotic system can be considered really autonomous only if procedures for emulating cognition are available, e.g., recognizing an observed object among a set of CAD models stored into a data base. In this case, the artificial vision process can be referred to as *high-level vision*.

Bibliography

Scientific literature on actuating systems and sensors is wide and continuously updated. The mechanical aspects on the joint actuating systems can be probed further in e.g. [186]. Details about electric servomotors can be found in [22], while in [156] construction and control problems for hydraulic motors are extensively treated. Control of electric drives is discussed in [128]; for direct drives see [12]. Joint control problems are discussed in [89].

A wide and detailed survey on sensors and in particular on proprioceptive sensors is given in [81]. In [220] force sensors are accurately described, with special attention to wrist force sensors. Further details about range sensors, with reference to mobile robotics applications, are available in [210]. Finally, a general introduction on vision sensors is contained in [48], while in [233] one of the most common calibration techniques for vision systems is described.

Problems

5.1. Prove (5.7)–(5.10).

5.2. Consider the DC servomotor with the data: $I_m = 0.0014\,\text{kg}\cdot\text{m}^2$, $F_m = 0.01\,\text{N}\cdot\text{m}\cdot\text{s/rad}$, $L_a = 2\,\text{mH}$, $R_a = 0.2\,\text{ohm}$, $k_t = 0.2\,\text{N}\cdot\text{m/A}$, $k_v = 0.2\,\text{V}\cdot\text{s/rad}$, $C_i G_v = 1$, $T_v = 0.1\,\text{ms}$, $k_i = 0$. Perform a computer simulation of the current and velocity response to a unit step voltage input V_c'. Adopt a sampling time of 1 ms.

5.3. For the servomotor of the previous problem, design the controller of the current loop $C_i(s)$ so that the current response to a unit step voltage input V_c' is characterized by a settling time of 2 ms. Compare the velocity response with that obtained in Problem 5.2.

5.4. Find the control voltage/output position and reaction torque/output position transfer functions for the scheme of Fig. 5.6.

5.5. For a Gray-code optical encoder, find the interconversion logic circuit which yields a binary-coded output word.

5.6. With reference to a contact situation of the kind illustrated in Fig. 5.16, let

$$\boldsymbol{r}_{cs}^{c} = [\,-0.3 \quad 0 \quad 0.2\,]^T\ \text{m} \qquad \boldsymbol{R}_{s}^{c} = \begin{bmatrix} 0 & 0 & 1 \\ 0 & -1 & 0 \\ 1 & 0 & 0 \end{bmatrix}$$

and let the force sensor measurement be

$$\boldsymbol{f}_{s}^{s} = [\,20 \quad 0 \quad 0\,]^T\ \text{N} \qquad \boldsymbol{\mu}_{s}^{s} = [\,0 \quad 6 \quad 0\,]^T\ \text{N}\cdot\text{m}.$$

Compute the equivalent force and moment in the contact frame.

5.7. Consider the SCARA manipulator in Fig. 2.34 with link lengths $a_1 = a_2 = 0.5\,\text{m}$. Let the base frame be located at the intersection between the first link and the base link with axis z pointing downward and axis x in the direction of the first link when $\vartheta_1 = 0$. Assume that a CCD camera is mounted on the wrist so that the camera frame is aligned with the end-effector frame. The camera parameters are $f = 8\,\text{mm}$, $\alpha_x = 79.2\,\text{pixel/mm}$, $\alpha_y = 120.5\,\text{pixel/mm}$, $X_0 = 250$, $Y_0 = 250$. An object is observed by the camera and is described by the point of coordinates $\boldsymbol{p} = [\,0.8 \quad 0.5 \quad 0.9\,]^T\,\text{m}$. Compute the pixel coordinates of the point when the manipulator is at the configuration $\boldsymbol{q} = [\,0 \quad \pi/4 \quad 0.1 \quad 0\,]^T$.